RSC Advances

PAPER

View Article Online
View Journal | View Issue

Cite this: *RSC Adv.*, 2025, **15**, 5523

$FeCl_3/SiO_2$-catalyzed bis-indolylation of acetals and ketals: a highly atom-economical approach to the selective deprotection of protected carbohydrates†

Barnali Das, Kamal Das, Utpal Ch. De and Swapan Majumdar *

A simple and green catalytic system is developed for the synthesis of 3,3′-bisindolyl(methanes) (BIMs) using cyclic/acyclic acetals as the carbon source for the bridging residue between two indole motifs. The reaction occurred under mild and benign conditions using $FeCl_3/SiO_2$ as a heterogeneous catalyst without the requirement of any toxic organic solvents. The ready availability and recyclability of the catalytic system allows the reaction to be highly efficient, resulting in very good BIM products. DFT studies were also performed to establish the proposed mechanism and preferential formation of unsymmetrical bisindolylmethanes using equimolar amounts of different indoles. The present protocol is also extended to the bisindolylation-induced selective cleavage of protected carbohydrates to diols in a 100% carbon-preservation and maximized atom-economical manner.

Received 2nd November 2024
Accepted 3rd February 2025

DOI: 10.1039/d4ra07809h

rsc.li/rsc-advances

Introduction

Nitrogen heterocycles are one of the most frequent scaffolds in pharmaceuticals. Amongst the various nitrogen heterocycles, the indole moiety is regarded as a privileged structure with potential applications in the field of agro- and medicinal chemistry. When properly functionalized, indoles can exhibit a wide range of pharmacological properties.[1] In particular, 3,3′-bis indolylmethanes (BIMs), composed of two indole units, have been isolated from marine and terrestrial natural sources,[2] such as plants, sponges, parasitic bacteria, and tunicates that include arundine, vibrindole A, streptindole, arsindoline A and B, turbomycin A and B, barakacin, annonidine B and dalesindole (Fig. 1). Due to the importance of BIM derivatives in the development of novel bioactive molecules, numerous synthetic methods to prepare this class of compounds have been reported.[3] The most exploited method for the synthesis of BIMs is the condensation of indoles with various aldehydes and ketones (Ehrlich test of indole), which is largely catalyzed by either protic or Lewis acids and seems to be straightforward and practical.[4] Accordingly, various protic or Lewis acid-catalyzed syntheses of bis(indolyl)methanes using indoles (2 equivalents) and carbonyl compounds (1 equivalent) have been reported in the literature.[5–25] The use[26] of 3-substituted indolyl alcohols and substituted indoles, metal-catalyzed carbonylation and alkylation reactions,[27] and metal-free oxidative reactions[28] have been adopted for the synthesis of BIMs. In the recent past, several efforts have also been devoted towards the synthesis of BIMs using substituted indoles with aryl amines,[29] benzyl amines,[30] and benzyl alcohols[31] as the second component in the condensation protocols. The synthesis of various symmetrical and unsymmetrical BIMs *via* the reaction of (3-indolylmethyl) trimethyl-ammonium iodides with a wide range of substituted indole derivatives has been reported.[32] The use of C1 and C2 alcohols as the carbon source for the bridging methylene group in BIMs under CuO-peroxymonosulfate (CuO-PMS) catalytic systems[33] and N-heterocyclic iodo(azo)lium salt organocatalytic protocols for the promotion of Friedel–Crafts-type reactions between indoles and aldehydes leading to the formation of BIMs has also been reported.[34] Despite having some advantages of their own, most of the reported methods indicate that the catalysts commonly used for such transformations are generally associated with one or more disadvantages, such as high toxicity, high cost, difficulty of handling, low thermal stability, and non-recyclability after being used.

The protection–deprotection technique is an important and desirable attribute in multi-step or target-oriented organic synthesis to prevent undesired/unwanted reactions. The carbonyls are generally protected as their acetal/ketal formation because of their easy incorporation as well as their survival in a wide range of reaction conditions.[35] Conversely, 1,2- and 1,3-diols in carbohydrate chemistry are usually protected by the formation of their isopropylidene or cyclohexylidene derivatives with acetone and cyclohexanone, respectively.[35,36] A significant

Department of Chemistry, Tripura University, Suryamaninagar, 799 022, India. E-mail: smajumdar@tripurauniv.ac.in; swamajumdar@gmail.com; swamajumdar@hotmail.com; Fax: +91-381-2374802; Tel: +91-381-237-9070; +91-8787793667; +91-9436124464

† Electronic supplementary information (ESI) available. See DOI: https://doi.org/10.1039/d4ra07809h

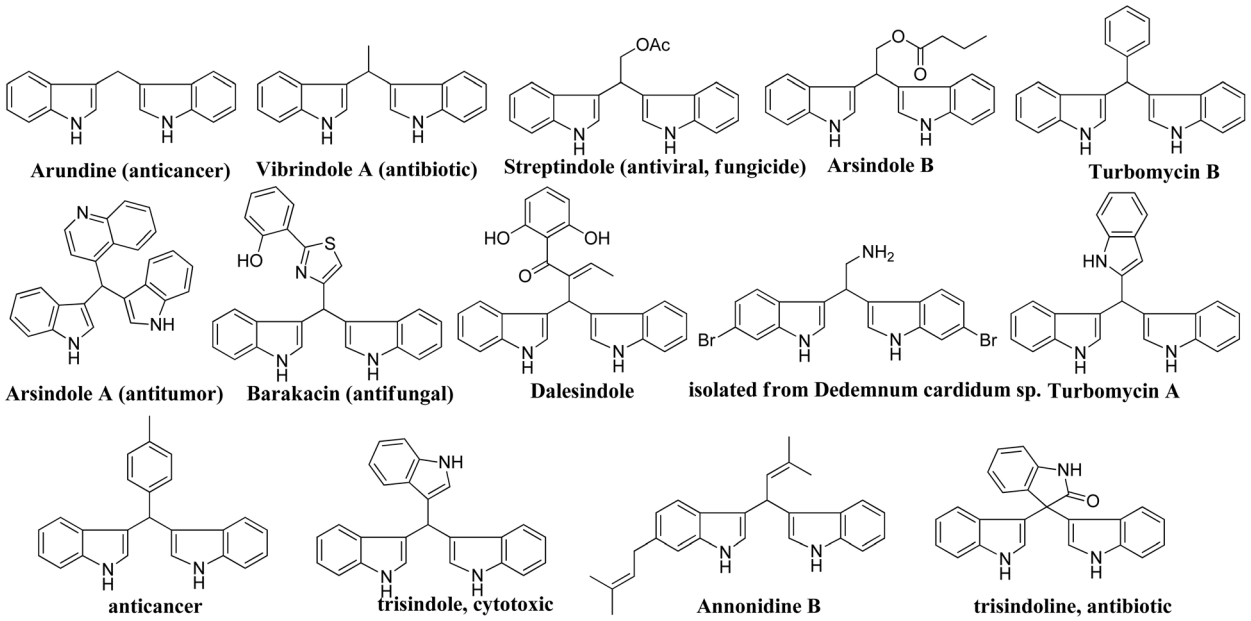

Fig. 1 Representative examples of biologically active natural/synthetic analogues of BIMs.

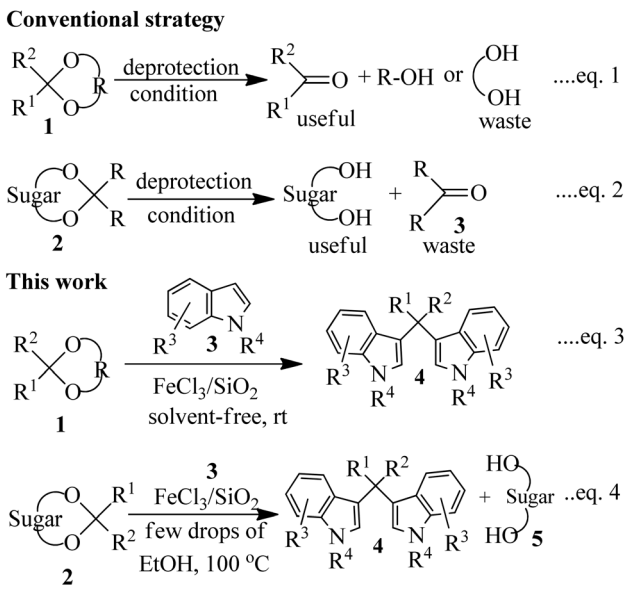

Scheme 1 Bis-indolylation-directed cleavage of acetals/ketals using silica-supported ferric chloride ($FeCl_3/SiO_2$) as a recyclable catalyst.

number of strategies for the deprotective cleavage of acetals, ketals, or other 1,3-dioxolanes that work in either acidic or non-acidic conditions are reported in the literature,[36] and usually either part of the protecting group goes to waste (Scheme 1, eqn (1) and (2)).

Iron(III) chloride is extensively used in organic synthesis as an ideal Lewis acid as it is an inexpensive and convenient reagent.[37] $FeCl_3 \cdot 6H_2O$ in association with ionic liquid or iron with Pd-catalyst one-pot domino reactions for the construction of bis(indolyl)methanes has been reported.[38–40] However, this reagent cannot be recycled after its use, which creates pollution issues. In recent years, the use of silica-supported catalysts has received considerable attention in organic syntheses because of enhanced activity, easier handling, recovery of the catalyst, low cost, and simple work-up procedure. Based on these features of supported reagents as heterogeneous catalysts, we[23,41] and others[42] utilized silica-supported ferric chloride ($FeCl_3/SiO_2$) as an activator for functional groups, which was utilized successfully in various organic transformations. It was reported that the acetal group can be activated by ferric chloride[43] or other transition metal catalysts[44] for the synthesis of heterocycles and other purposes under mild conditions. For several years, we were actively engaged in the development of newer methodologies[45a–f] for the synthesis of potential bioactive compounds, and in continuation of our efforts towards the development of benign protocols, we hereby report a novel and efficient method for the preparation of bis-indolylmethane derivatives (BIMs) *via* multi-component assembly of electrophilic substitution reactions of indoles with acetal-protected carbonyls in the presence of silica-supported ferric chloride ($FeCl_3/SiO_2$) as a recyclable and eco-friendly catalyst (eqn (3), Scheme 1). We also extended this methodology for the first time towards a selective bis-indolylation-directed deprotection of isopropylidene/cyclohexylidene-protected carbohydrate to the corresponding diol under anhydrous conditions in a highly atom-economical manner (eqn (4), Scheme 1).

Results and discussion

For optimization of reaction conditions and yield of bis-indolylmethanes (**4a**), we began with benzaldehyde dimethylacetal (**1a**) and indole (**3a**) as model substrates using different catalysts that are known to activate acetals under solvent-free conditions. No product was obtained upon grinding of **1a** and **3a** in a 1 : 2 molar ratio in the absence of catalyst (Table 1, entry

Table 1 Optimization of BIM (**4a**) synthesis from benzaldehyde dimethyl acetal (**1a**) and indole (**3a**)

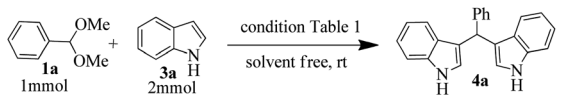

Entry	Catalyst	Temp. (°C)	Time (min)	Yield (%)
1	No	rt	180	No reaction
2	No	80	30	Decomp
3	SiO_2	rt	180	40
4	$FeCl_3$	rt	30	Mixture
5	$FeCl_3$–SiO_2 (20 mg)	rt	15	90
6	$FeCl_3$–SiO_2 (50 mg)	rt	15	90
7	$FeCl_3$–SiO_2 (10 mg)	rt	15	80
8	Nano TS 1 (10 mg)	rt	15	55
9	$HClO_4$–SiO_2 (20 mg)	rt	15	70
10	PANI-$FeMnO_4$ (10 mg)	rt	180	Mixture
11	Amberlite IR120 (20 mg)	rt	180	83
12	[HBIm]TFA (20 mg)	70	120	70
13	[BMIm]Br (20 mg)	70	180	Trace

1), but on heating at 80 °C, decomposition of the materials was detected on a TLC plate (Table 1, entry 2). Grinding the mixture of **1a** and **3a** by keeping their ratios the same with SiO_2 (230–400 mesh, 20 mg) for 3 h, **4a** was isolated in 40% yield (Table 1, entry 3) along with the recovery of unreacted indole. Considering the Lewis acid character of $FeCl_3$, we employed 5 mol% of $FeCl_3$ while grinding the mixture of **1a** and **3a** (1 : 2 molar ratio). Unfortunately, this failed to produce any isolable product from the reaction mixture after 30 min as multiple spots were detected on the TLC plate. Then, based on our previous work,[46] we decided to explore the catalytic potentiality of $FeCl_3/SiO_2$ (230–400 mesh was used) as an activator of acetal groups in our present work. We were pleased to observe that grinding the mixture with pre-prepared $SiO_2/FeCl_3$ (20 mg, containing 2 mol% of $FeCl_3$)[23] for 15 min results in a clean transformation of the substrates to the desired BIM **4a** in 90% yield (Table 1, entry 5). An increase in the amount of $SiO_2/FeCl_3$ (50 mg) does not improve the yield (Table 1, entry 6), but decreasing the amount of catalyst to 10 mg (1 mol% of $FeCl_3$) decreased the yield of **4a** to 80% (Table 1, entry 7). To evaluate the catalytic superiority of silica-supported ($FeCl_3/SiO_2$), we screened other supported/heterogeneous catalysts such as Nano TS-1, silica-supported perchloric acid, magnetic PANI-$FeMnO_4$, and Amberlite IR 120H^+ for the indolylation reaction. However, these catalysts provided inferior results (Table 1, entries 8–11) compared to the $SiO_2/FeCl_3$-catalyzed reaction (Table 1, entry 5). In the case of PANI-$FeMnO_4$, a complex mixture was detected using thin-layer chromatographic techniques. We also screened imidazolium-based ionic liquids, such as 1-butyl imidazolium trifluoroacetate and 1-butyl-3-methylimidazolium bromide, under solvent-free homogenous conditions at 80 °C. We have previously reported that the protic ionic liquid 1-butyl imidazolium trifluoroacetate could be an effective medium for the hydrolytic cleavage of acetals/ketals at 70 °C.[45a] During the investigation, we found that this protic ionic liquid provided a 70% yield of **4a** after 2 h. In contrast, the neutral ionic liquid 1-butyl-3-methylimidazolium bromide provided a trace amount of **4a** after 3 h.

With the optimized conditions in hand (Table 1, entry 5), we decided to explore the substrate scope and efficacy of the present procedure. For this, a wide variety of protected carbonyls (**1**) were allowed to react with various indoles (**3**) under standard conditions. Overall, the reaction conditions were found to be general. The reaction of benzaldehyde dimethyl acetal (**1a**) with *N*-methyl indole (**3b**) and 2-methyl indole (**3c**) in the presence $FeCl_3/SiO_2$ under solvent-free conditions at room temperature furnished the desired bisindolylated products **4b–c** in high yields (92 and 91%, respectively); however, in the case of an electronically crowded 2-phenyl indole (**3d**), only 84% yield of the desired product was obtained (Table 2, entries 2–4). The ability to tolerate a halide that is present in the indole ring (**3e**) also demonstrated the efficacy of the protocol is general, although with a slightly lower yield of the expected product (Table 2, entry 5). The present protocol is compatible with methoxy substituents present in either of the coupling partners. The methoxy group present in the indole ring (**3f**) provided a better yield with protected benzaldehyde (**1a**) than the dimethylacetal functionalized anisole (**1b**) with simple indole (**3a**) (Table 2, entries 6 and 7). The electron-withdrawing nitro group present in the *o*- and *p*-positions of the benzaldehyde diethyl acetal (**1c–d**) reacted well with a simple indole (**3a**) or a 1-methyl indole (**3b**), producing an excellent yield of the expected products **4h–k** (Table 2, entries 8–11), but the reaction lasted longer compared to entries 1–7 in Table 2. The reaction works well but slowly when a nitro group is present in the indole moiety (Table 2, entry 12). It was noticed that the acetal generated from ketones such as 2,2-dimethoxy propane (acetone dimethyl acetal; **1e**) and cyclohexanone dimethyl acetal (**1f**) underwent a smooth bisindolylation reaction with the indole/substituted indole, achieving a very good-to-excellent yield of **4m–p** (Table 2, entries 13–16). Notably, the treatment of triethyl orthoformate under similar reaction conditions using three equivalents of the indole results in a clean transformation, producing a very high yield of tris-indolyl methane (**4q**) after 60 minutes (Table 2, entry 17). The present procedure was also shown to proceed well for 2-phenyl 1,3-dioxolane (**1h**) and 2-(4-chlorophenyl) 1,3-dioxolane (**1i**) with the indole, producing bis-indolyl derivatives **4a** and **4r** in good yield (Table 2, entries 18 and 19). In spite of the present methodology for bisindolylation of acetals/ketals having a broad functional group tolerance, the present protocol failed to produce the product when a strong electron-withdrawing group was present in the α-position of the dimethyl acetal-protected aldehyde (Table 2, entries 20 and 21). Based on our recent report[46] on the synthesis of multisubstituted imidazole *via* $FeCl_3/SiO_2$-catalyzed activation of acetals, we postulated the mechanism, which is depicted in Fig. 2. We believe that the iron of $FeCl_3/SiO_2$ coordinates with both the oxygens of acetal and facilitates the formation of an intermediate oxonium ion (**B**) after expulsion of the alkoxide ($R'O^-$). Then, the indole acts as a nucleophile to attack the highly reactive oxonium ion **B** *via* the C-3 position of the indole ring to produce the intermediate **C**,

Table 2 Scope and generality of the $SiO_2/FeCl_3$-catalyzed synthesis of bisindoles using indoles and protected carbonyl compounds

Entry	Protected carbonyl	Indole	Product	Time (min)	Yield (%)
1	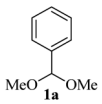		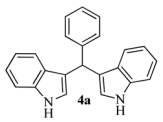	15	90
2	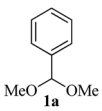		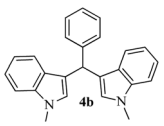	15	92
3	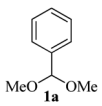	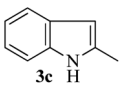	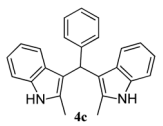	15	91
4	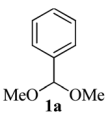	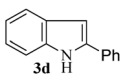	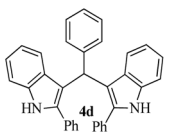	30	84
5	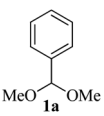	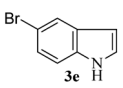	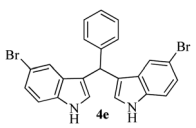	30	85
6	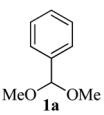	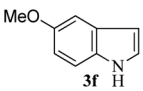	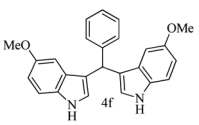	30	90
7	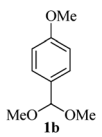	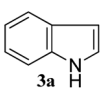	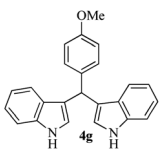	30	85
8	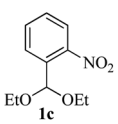	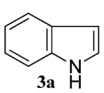	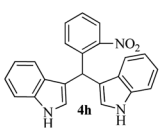	90	93
9	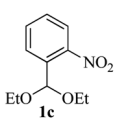	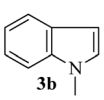	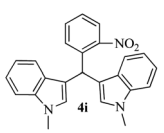	90	91
10	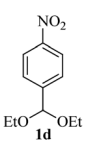	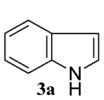	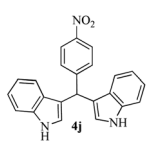	90	87
11	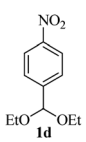		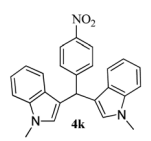	90	82
12	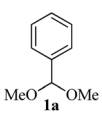	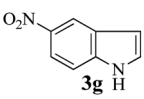	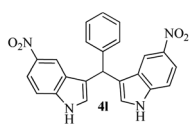	60	82
13				30	95

Table 2 (*Contd.*)

Entry	Protected carbonyl	Indole	Product	Time (min)	Yield (%)
	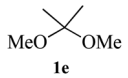 1e	 3a	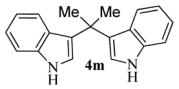 4m		
14	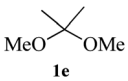 1e	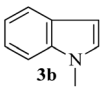 3b	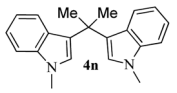 4n	30	86
15	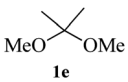 1e	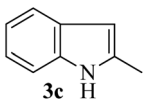 3c	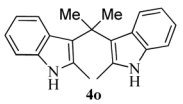 4o	30	83
16	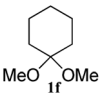 1f	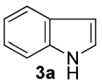 3a	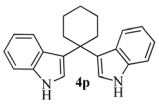 4p	30	85
17	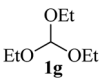 1g	 3a	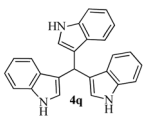 4q	60	91
18	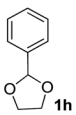 1h	 3a	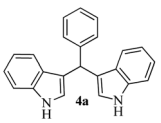 4a	45	86
19	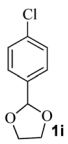 1i	 3a	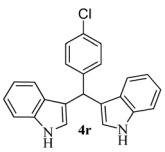 4r	45	86
20	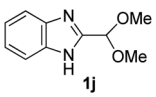 1j	 3a	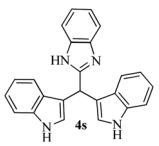 4s	60	NR
21	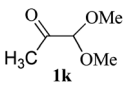 1k	 3a	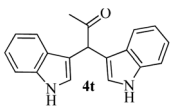 4t	60	NR

which, upon subsequent release of a proton and aromatization, gives another intermediate **D**. Due to the allylic ether nature of the intermediate **D**, it is further activated by $FeCl_3/SiO_2$ to yield the highly reactive azafulvene-type intermediate **E** *via* the indole through an N-triggered elimination of $R'O^-$. This reactive intermediate **E** invites a second molecule of indole to participate in the Michael addition reaction to afford **F**. Removal of a proton and release of the catalyst produces bis-indolylmethane **4**. Notably, the involvement of the initial formation of the carbonyl compound *via* hydrolytic cleavage by the catalysis of $FeCl_3$ is excluded, as evident from the NMR experiment. A solution of **1d** (10 mg) in DMSO-d_6 (0.6 mL) was placed in an NMR tube and then the ^{1}H NMR spectrum was recorded in the presence of $FeCl_3/SiO_2$ at ambient temperature after 15 min. No signal of an aldehydic functional group due to hydrolytic cleavage of diethyl acetal group in **1d** was detected.

However, the broadening of some signals was detected when such spectra were recorded with a suspension of silica-supported $FeCl_3$. Unsuccessful attempts (Table 2, entries 20 and 21) using benzimidazole 2-carboxaldehyde dimethyl acetal and pyruvaldehyde dimethyl acetal also support our hypothesis, as the corresponding intermediate oxonium (**B**) is unstable due to the electron-withdrawing ability of the attached residue. It was also reported that pyruvaldehyde itself undergoes a bis-indolylation reaction in the presence of pTSA with indole,[11] so if hydrolytic cleavage occurred by $FeCl_3/SiO_2$, there would have

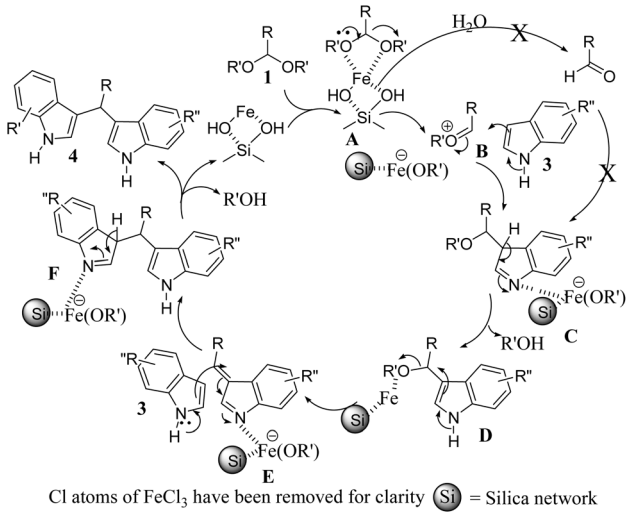

Fig. 2 Proposed reaction mechanism of the $FeCl_3/SiO_2$-catalyzed bis-indolylation of an acetal.

been the possibility to isolate bisindole **4t** from the reaction of pyruvaldehyde dimethyl acetal and indole. The formation and stability of the intermediate **E** depend on the substituent present in the indole ring. The electron-donating substituents in indole favor the formation of **E**; in contrast, strong electron-withdrawing groups, such as a nitro group, destabilize it to some extent. By taking advantage of the substituent control formation of **E**, it is possible to control the preferential synthesis of unsymmetrical BIMs. For example, the reaction of benzaldehyde dimethyl acetal (**1a**) with indole (**3a**) and 5-methoxy indole (**3f**) in a ratio of 1 : 1 : 1 under standard conditions produced the unsymmetrical bis-indolyl methane (**4u**) as the major product (54%), along with symmetrical bisindole **4a** (24%) and **4f** (18%) (Scheme 2, eqn (1)). Interestingly, the use of **1a** : **3a** : **3f** in a 1 : 1 : 2 ratio produces **4f** exclusively, but if we change the ratio to 1 : 2 : 1 again, **4u** remains the major product (50%). We have also conducted a study using other acetals such as **1d** and **1g** with a simple indole **3a** and reactive indoles **3f** or **3b**. Using equimolar ratios of **1d**/**3a**/**3f** provided the cross product **4v** (70%) as the major product along with 23% of **4j** and a trace amount of **4w**. Similarly, unsymmetrical bis-indolyl methane **4x** was formed as the major product (51%) when **1g**/**3a**/**3b** was employed in a 1 : 1 : 1 ratio. In all cases, each of the products was purified by column chromatography using ethyl acetate and hexanes (1 : 9 to 1 : 1) and then quantified based on the amount of isolated pure products. The preferential formation of unsymmetrical bis-indolylmethanes, as shown in Scheme 2, could be explained by the relative stability of the proposed intermediate **E** (Fig. 2) generated *in situ* from indoles and aldehydes. The overall reaction may be considered as a thermodynamically controlled (formation of the intermediate **E**) first step, followed by a kinetically controlled nucleophilic attack of a second indole molecule, leading to the formation of

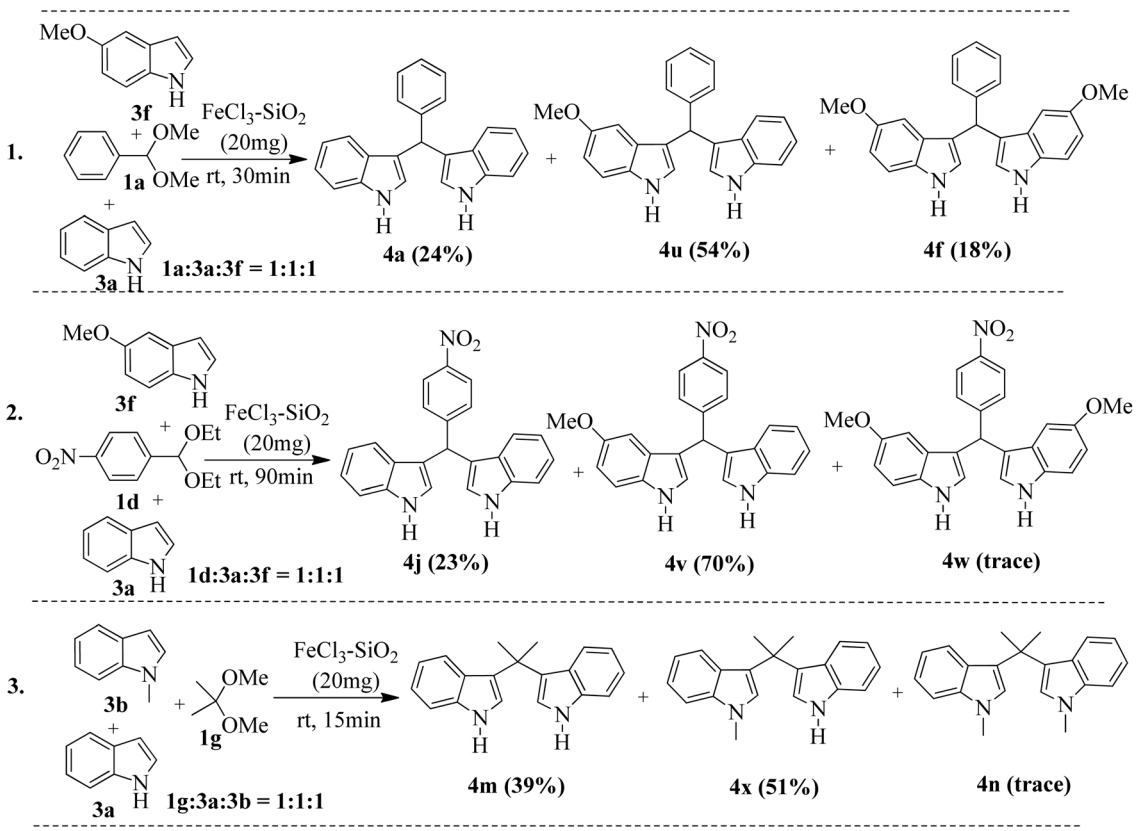

Scheme 2 Control experiments for the synthesis of unsymmetrical bis-indolylmethanes.

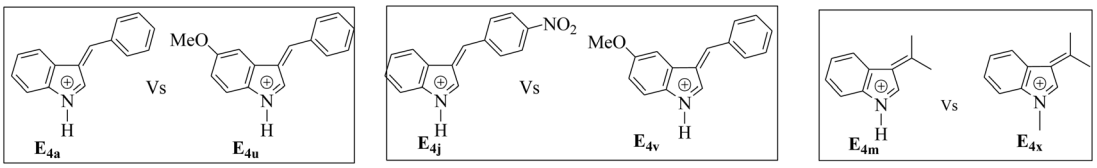

Fig. 3 Structure of various proposed intermediates in Scheme 2.

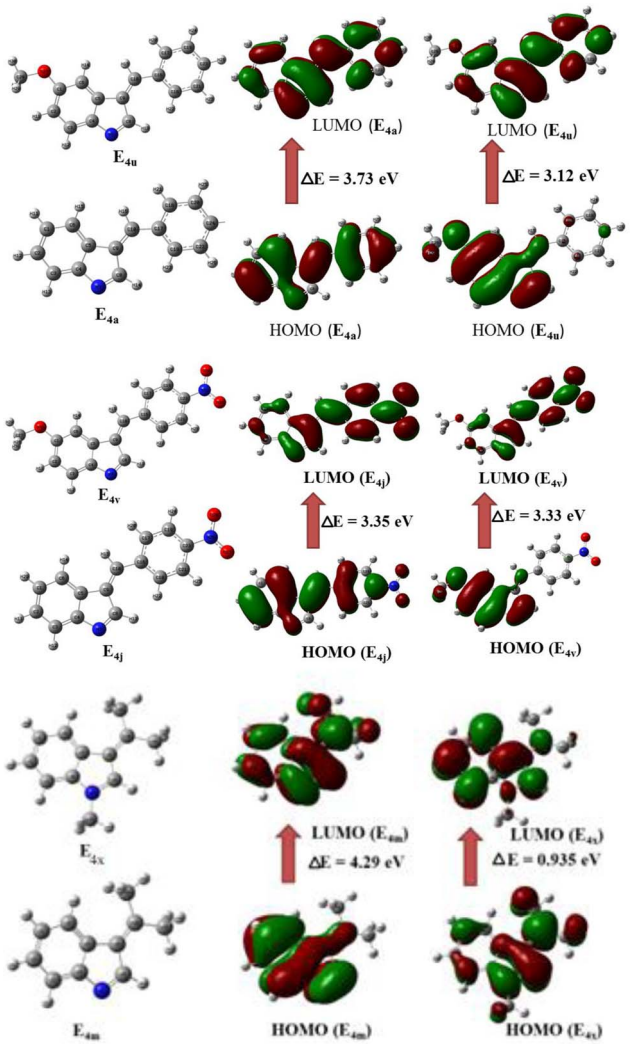

Fig. 4 Optimized structures of intermediates of Fig. 3 and their HOMO–LUMO energy gaps.

final products. The electron-donating substituent (–OMe) present in the indole ring of the intermediate $\mathbf{E_{4u}}$ stabilizes it over $\mathbf{E_{4a}}$, and thus **4u** becomes the major product after the kinetically controlled addition of the second indole molecule to $\mathbf{E_{4u}}$. Symmetrical BIM **4f** becomes the minor product due to the low quantity (mostly used in the first step) of **3f** [Scheme 2(**1**)]. Similarly, **4v** and **4x** are the major products; **4j** and **4m** are minor, and **4w** and **4n** are formed in trace amounts, as shown in Scheme 2(**2**) and 2(**3**), respectively. Therefore, the results indicated that the stability of $\mathbf{E_{4v}} > \mathbf{E_{4j}}$ and $\mathbf{E_{4x}} > \mathbf{E_{4m}}$. Thus, the outcome of the reaction indicated the highly competitive nature of the condensation process during the course of the reactions. To justify our hypothesis, we performed quantum mechanical calculations to assess the relative stability of all the proposed intermediates for $\mathbf{E_{4a}}$ *vs.* $\mathbf{E_{4u}}$, $\mathbf{E_{4j}}$ *vs.* $\mathbf{E_{4v}}$ and $\mathbf{E_{4m}}$ *vs.* $\mathbf{E_{4x}}$ (Fig. 3) using Density Functional Theory (DFT) with B3LYP/6311G(d,p) in Gauss 16w software.[47] Energy optimization in the DFT study of the proposed intermediates (Fig. 3) predicted that the total energy (TE) of intermediate pairs *viz.* $\mathbf{E_{4a}}/\mathbf{E_{4u}}$, $\mathbf{E_{4j}}/\mathbf{E_{4v}}$, and $\mathbf{E_{4m}}/\mathbf{E_{4x}}$ was −632.4196 and −746.9743, −837.6709 and −952.1623, and −479.9631 and −519.8499 Hartree, respectively, suggesting the thermodynamic stabilities as $\mathbf{E_{4a}} < \mathbf{E_{4u}}$, $\mathbf{E_{4j}} < \mathbf{E_{4v}}$, and $\mathbf{E_{4m}} < \mathbf{E_{4x}}$. Herein, the observed low energy value of the corresponding optimized structures (Fig. 4) of the stable intermediates ($\mathbf{E_{4u}}$ and $\mathbf{E_{4v}}$) having an electron-donating group (–OMe) may be attributed to the conjugation of electrons favoring the stabilities. However, in the case of $\mathbf{E_{4m}}$ and $\mathbf{E_{4x}}$, hyperconjugative electron delocalization of the $-CH_3$ group attached to the indole nitrogen atom might favor $\mathbf{E_{4x}}$ in making it more stable than $\mathbf{E_{4m}}$. In addition, the HOMO–LUMO (HL) gap, as an index of kinetic stability (a low gap indicates greater stability),[48,49] supports the stabilities of $\mathbf{E_{4u}}$ in $\mathbf{E_{4a}}/\mathbf{E_{4u}}$ (3.73/3.12 eV) and $\mathbf{E_{4v}}$ in $\mathbf{E_{4j}}/\mathbf{E_{4v}}$ (3.35/3.33 eV) pairs. Moreover, a close HL gap (Fig. 4) of the intermediates in each pair, particularly in $\mathbf{E_{4a}}/\mathbf{E_{4u}}$ and $\mathbf{E_{4j}}/\mathbf{E_{4v}}$, suggests that the second step of the reactions, *viz.* nucleophilic attack of the second indole, is kinetically controlled and almost equally probable. In the case of $\mathbf{E_{4m}}$ and $\mathbf{E_{4x}}$, the comparatively very low HL gap in $\mathbf{E_{4x}}$ (0.935 eV) compared to $\mathbf{E_{4m}}$ (4.29 eV) indicated that $\mathbf{E_{4x}}$ has the highest thermodynamic stability (low TE) as well as kinetic stability compared to $\mathbf{E_{4m}}$. Therefore, this report of bis-indolylation reactions is mainly driven by the thermodynamic stability of the concerned *in situ* intermediates, which, in turn, is governed by the presence or absence of electron-donating substituents in the intermediates. The optimized structures of intermediates (Fig. 3) and their HOMO–LUMO energy gaps are shown in Fig. 4.

After the successful accomplishment of this new synthetic strategy for the synthesis of bis-indolylmethanes from acetal-/ketal-protected carbonyls with a wide range of indoles using silica-supported ferric chloride, we were curious to observe the reactivity of the same catalyst against the acetal-protected carbohydrates. The hydrolytic deprotection of acetal-protected sugar, generally a ketone (eqn (2) in Scheme 1), goes to waste. Their isolation from the post-reaction mixture is difficult or not

Table 3 Scope and generality of the $SiO_2/FeCl_3$-catalyzed bisindolylation-induced selective deprotection of protected sugar at 100 °C

Entry	Protected sugar	Indole	Time (h)	Products (yield, %)
1	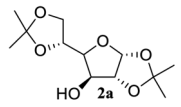	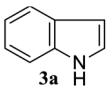	1.0	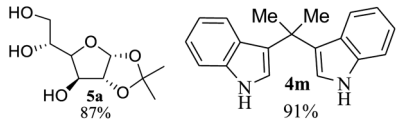
2	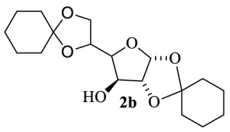	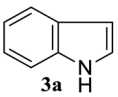	1.0	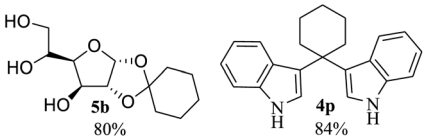
3	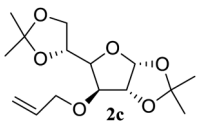	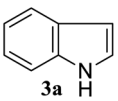	1.5	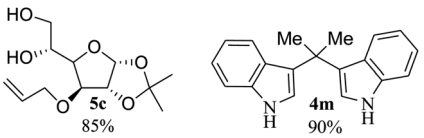
4	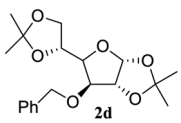	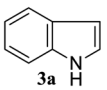	1.0	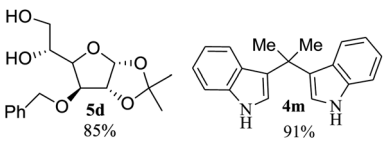
5	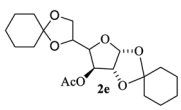	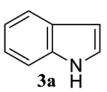	1.0	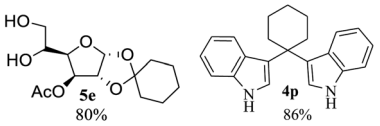
6	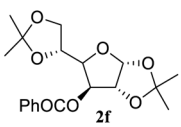	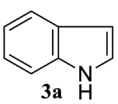	1.0	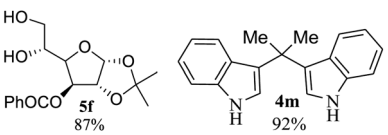
7	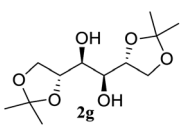	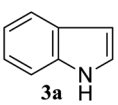	3.0	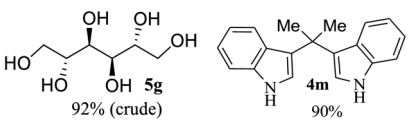
8	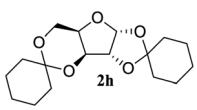	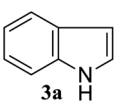	1.0	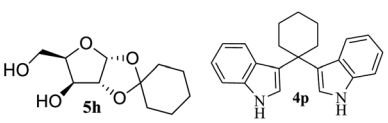
9	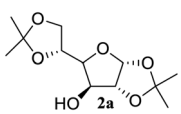	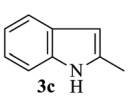	1.0	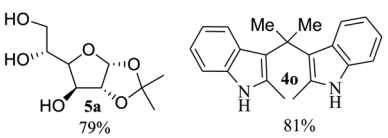
10	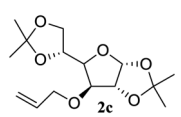	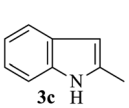	1.5	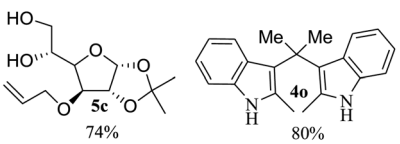

valued due to their volatile nature and high solubility in water. The unusual findings assembled in Table 2 indicate that the carbonyl part of acetals/ketals (**1**) appeared in the bridged carbon of bisindole derivatives (**4**), while the alcoholic residue (eqn (3), Scheme 1) was eliminated as waste. As the results shown in Table 2 are very interesting, this prompted us to explore the possibility of the selective activation–deprotection of isopropylidene or cyclohexylidene groups present as protecting groups in carbohydrate derivatives, since this could be a viable route for a 100% atom-economical strategy for the

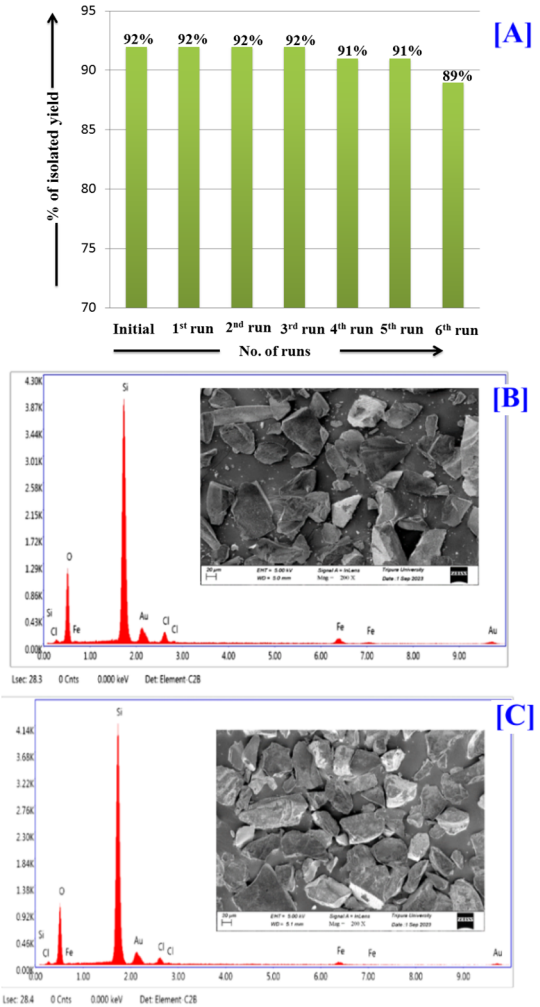

Fig. 5 (A) Results of the recyclability test of the catalyst $FeCl_3/SiO_2$; (B) SEM image and EDAX spectra of the freshly prepared catalyst; (C) SEM image and EDAX spectra of the recycled catalyst (after the 6th cycle).

deprotection of protected carbohydrates under benign conditions. Thus, we began with 1,2:5,6-di-*O*-isopropylidene glucofuranose (**2a**) as a protected substrate and two equivalents of indole (**3a**) to screen with silica-supported ferric chloride ($FeCl_3/SiO_2$) for the cleavage of 1,3-dioxolane in a non-aqueous medium under standard conditions (Table 1, entry 5). Our initial attempt at room temperature failed to produce any cleavage product; however, conducting the reaction at elevated temperatures (95–100 °C) for 1 h in the presence of a small amount of methanol or ethanol (~0.3 mL) resulted in complete conversion, and bis-indole **4m** and the 5,6-deprotected product **5a** were produced in 91% and 87% isolated yield, respectively (Table 3, entry 1), after column chromatographic separation. Similarly, the selective deprotective bis-indolylation of 1,2:5,6-di-*O*-cyclohexylidene glucofuranose (**2b**) with indole (**3a**) also afforded the bis indole (**4p**) and 1,2-*O*-cyclohexylidene glucofuranose (**5b**) in 84% and 80% isolated yield, respectively, under similar reaction conditions (Table 3, entry 2). It is worth mentioning here that a large amount of 75% AcOH in water is the reagent of choice for the selective cleavage of 5,6-*O*-isopropylidene or cyclohexylidene groups in carbohydrate scaffolds,[50] which makes the process less economical, laborious, and not eco-friendly, as the use of toluene is essential to removing acetic acid from the product. With this, we realized that the present bis-indolylation of protected carbohydrate could be a general procedure for the selective deprotection of orthogonally protected sugar with 100% atom economy that allows 100% carbon preservation as well. Therefore, to determine the generality of the procedure, each of the protected carbohydrate derivatives **2c–f** and different indoles was subjected to treatment with $FeCl_3/SiO_2$ (20 mg) in 0.3 mL of ethanol (to facilitate the stirring) at 80 °C (Table 3). Protected carbohydrates **2c–f** produced the corresponding 5,6-deprotected products in excellent yield with simple indoles in a regioselective manner. The functional groups present in di-*O*-isopropylidene or di-*O*-cyclohexylidene hexose, such as allyl, benzyl, acetyl, and benzoyl groups, survived under the reaction conditions with concomitant formation of bis-indolyl methanes (**4m** and **4p**). The yield of each deprotected sugar and bis-indolyl methanes (**4m** and **4p**) is given in Table 3 (entries 3–6). In all cases, the 1,2-*O*-isopropylidene or 1,2-*O*-cyclohexalidene groups remain intact, as revealed by the NMR spectra of the products. However, in the case of 1,2:5,6-di-*O*-isopropylidene-D-mannitol, complete deprotection was witnessed, and for clean conversion, 4.0 equivalents of indole were needed (Table 3, entry 7). The present protocol was also applicable to 1,2:3,5-di-*O*-cyclohexylidene xylofuranose. Under the reaction conditions, only the 3,5-*O*-protecting group was cleaved (Table 3, entry 8). The selective deprotection of protected hexose is general for other indoles as well; for instance, 2-methyl indole can efficiently convert protected sugars **2a** and **2c** to the corresponding diol **5a** and **5c** in 79% and 74% yield, respectively. In each entry (Table 3, entries 9 and 10), 3,3′-(propane-2,2-diyl)bis(2-methy-1*H*-indole) (**4o**) was formed in approx. 80% yield.

Finally, we turned our attention to the recyclability of the catalyst $SiO_2/FeCl_3$ used in the bis-indolylation reaction. The recyclability of the catalyst was investigated by recovering the catalyst $FeCl_3/SiO_2$ (20 mg) from the reaction of 1-methyl indole (**3b**, 2 mmol) and benzaldehyde dimethyl acetal (**1a**, 1.0 mmol) (Table 2, entry 2). After the completion of the reaction (15 min, TLC), the mixture was dissolved in ethyl acetate (5.0 mL) and filtered out through the filter paper. The residue was then washed thoroughly with ethyl acetate (~5 mL) until no residual product was left. The combined filtrate was concentrated and recrystallized from ethyl acetate–hexane (1 : 1) to obtain pure product (**4b**). The residue catalyst was collected from the filter paper, dried under vacuum, weighed, and was used for the next cycle. The weight loss of the catalyst was found to be negligible. The recyclability tests were performed six times in a similar manner, and our results (Fig. 5A) showed that the catalyst retained its activity (92% initially, 92%, 92%, 92%, 91%, 91%, and 89%). We also checked the SEM images and EDAX of the catalyst before and after recycling to see if any morphological changes occurred during its handling in multiple cycles. SEM micrographs of $FeCl_3/SiO_2$ (230–400 mesh) show that the particles were random in size and shape and well dispersed. An EDX spectrum of the catalysts confirmed the presence of Si, O,

Cl, and Fe elements, suggesting the formation of the $FeCl_3/SiO_2$ catalytic system. Similarly, an SEM image of the recycled $FeCl_3/SiO_2$ catalyst (after six cycles) was compared with the original images. However, we did not notice any significant differences in morphology and EDAX of the recycled one with the original images (Fig. 5B and C).

Conclusions

A simple, green, and recyclable catalytic system was developed for the synthesis of 3,3′-bisindolyl(methanes) (BIMs) *via* the diindolylation of cyclic/acyclic acetals. The reaction occurred under mild and benign conditions using $FeCl_3/SiO_2$ as a heterogeneous catalyst without the requirement of any toxic organic solvents. This method relied on a wide range of acetals—aromatic, aliphatic, or carbohydrates—resulting in excellent-to-very-good yields of BIMs. DFT studies were also performed to establish the proposed mechanism and preferential formation of unsymmetrical bisindolylmethanes using equimolar amounts of different indoles. The present protocol was also extended to bisindolylation-induced selective cleavage of protected carbohydrates to diols in a 100% carbon-preservation and maximized atom-economical manner.

Experimental section

General procedure for the indolylation of acetals in the presence of $FeCl_3/SiO_2$ (ref. 23 and 46)

To a cone-shaped flask, the acetal (1.0 mmol), indole (2.0 mmol), and $FeCl_3/SiO_2$ catalyst (20 mg, 2 mol% of $FeCl_3$) were added (for the carbohydrate substrate, 0.2 to 0.3 mL of alcohol was needed). The reaction mixture was stirred for the stipulated time and temperature mentioned in Tables 2 and 3. After completion of the reaction, the reaction mixture was diluted with EtOAc (5 mL) and filtered. The filtrate was evaporated under vacuum. The desired product was isolated either by crystallization or by column chromatography using ethyl acetate–hexane (1 : 3 to 3 : 1).

Physical and spectral data of unknown BIMs

3,3′-((2-Nitrophenyl)methylene) bis(1-methyl-1*H*-indole) (4i). Yield: 91%, light yellow solid, mp. 160–162 °C; IR (KBr) ν_{max} 3052, 1514, 1467, 1339, 1120, 781 cm^{-1}; ^1H NMR (400 MHz, DMSO-d_6) δ 7.90 (d, $J = 8.0$ Hz, 1H), 7.58 (t, $J = 8.8$ Hz, 1H), 7.48 (t, $J = 7.6$ Hz, 1H), 7.41 (t, $J = 8$ Hz, 3H), 7.23 (d, $J = 7.6$ Hz, 2H), 7.13 (t, $J = 7.2$ Hz, 2H), 6.94 (t, $J = 7.6$ Hz, 2H), 6.80 (s, 2H), 6.40 (s, 1H), 3.71 (s, 6H); ^{13}C NMR (100 MHz, DMSO-d_6) δ 149.8, 138.1, 137.4, 133.1, 131.0, 128.9, 128.1, 127.0, 124.5, 121.8, 119.2, 119.1, 115.7, 110.3, 34.2, 32.8; HRMS calcd for ($C_{25}H_{21}N_3O_2 + H^+$) 396.1712, found: 396.1692 ($M + H^+$).

3,3′-(Propane-2,2-diyl)bis(1-methyl-1*H*-indole) (4n). Yield: 86%, white solid, mp. 130 °C; IR (KBr) ν_{max} 3744, 1463, 1322, 1225, 1049, 734 cm^{-1}; ^1H NMR (400 MHz, $CDCl_3$) δ 7.49 (d, $J = 8.4$ Hz, 1H), 7.30 (d, $J = 8.0$ Hz, 2H), 7.17 (t, $J = 8.4$ Hz, 1H), 6.96–6.93 (m, 2H), 3.78 (s, 3H), 1.96 (s, 3H); ^{13}C NMR (100 MHz, $CDCl_3$) δ 137.8, 126.7, 125.5, 124.1, 121.5, 120.9, 118.1,109.1, 35.0, 32.7, 31.0, 30.3 HRMS calcd for ($C_{21}H_{22}N_2 + H^+$) 303.1861, found: 303.1849 ($M + H^+$).

3,3′-(Propane-2,2-diyl)bis(2-methyl-1*H*-indole) (4o). Yield: 83%, white solid, mp. 130 °C; IR (KBr) ν_{max} 3378, 2310, 1546, 1453, 1340, 1014, 740 cm^{-1}; ^1H NMR (400 MHz, DMSO-d_6) δ 10.53 (s, 2H), 7.22 (d, $J = 8.0$ Hz, 2H), 7.16 (d, $J = 8.0$ Hz, 2H), 6.84 (t, $J = 7.6$ Hz, 2H), 6.67 (t, $J = 8.0$ Hz, 2H), 2.28 (s, 6H), 1.92 (s, 6H); ^{13}C NMR (100 MHz, DMSO-d_6) δ 135.4, 130.1, 128.2, 120.2, 119.6, 119.4, 118.0, 110.6, 37.7, 32.2, 14.5; HRMS calcd for $C_{21}H_{22}N_2$ 302.1783, found: 302.1747 (M^+).

3-((1*H*-Indol-3-yl)(phenyl)methyl)-5-methoxy-1*H*-indole (4u). Yield: 61%, off-white solid, mp. 156–158 °C; IR (KBr) ν_{max} 3404, 1484, 1206, 1018 cm^{-1}; ^1H NMR (400 MHz, $CDCl_3$) δ 7.93 (s, 1H), 7.83 (s, 1H), 7.42–7.20 (m, 10H), 7.03 (s, 1H), 6.86 (d, $J = 8.0$ Hz, 2H), 6.67 (d, $J = 12.0$ Hz, 2H), 5.86 (s, 1H); ^{13}C NMR (100 MHz, $CDCl_3$) δ 153.7, 144.0, 136.8, 131.8, 128.7, 128.2, 127.5, 127.1, 126.2, 124.4, 123.7, 121.9, 120.0, 119.6, 119.4, 119.2, 112.0, 111.7, 111.1, 101.9, 55.9, 40.3; HRMS calcd for ($C_{24}H_{20}N_2O$–H^+) 351.1497, found: 351.1516 ($M - H^+$).

3-((1*H*-Indol-3-yl)(4-nitrophenyl)methyl)-5-methoxy-1*H*-indole (4v). Yield: 70%, light yellow solid, mp. 180–182 °C; IR (KBr) ν_{max} 3448, 1501, 1341, 1201, 1062, 920, cm^{-1}; ^1H NMR (400 MHz, $CDCl_3$) δ 8.17 (d, $J = 8.8$ Hz, 2H), 8.06 (s, 1H), 7.95 (s, 1H), 7.52 (d, $J = 8.8$ Hz, 2H), 7.41 (d, $J = 8.0$ Hz, 1H), 7.42–7.28 (m, 3H), 7.22 (t, $J = 8.0$ Hz, 1H), 7.06 (d, $J = 8.0$ Hz, 1H), 6.89 (dd, $J = 6.4$, 2.4 Hz, 1H), 6.79 (d, $J = 2.4$ Hz, 1H), 6.71 (s, 1H), 6.67 (s, 1H), 5.96 (s, 1H), 3.73 (s, 3H); ^{13}C NMR (100 MHz, $CDCl_3$) δ 154.0, 151.8, 146.6, 136.8, 131.8, 129.5, 127.1, 126.7, 124.4, 123.7, 123.6, 122.3, 119.6, 118.0, 117.8, 112.3, 112.0, 111.3, 101.6, 76.7, 55.9, 40.2; HRMS calcd for ($C_{24}H_{19}N_3O_3 + H^+$) 398.1505, found: 398.1513 ($M + H^+$).

3-(2-(1*H*-Indol-3-yl)propan-2-yl)-1-methyl-1*H*-indole (4x). Yield: 51%, off-white solid, mp. 102–104 °C; IR (KBr) ν_{max} 3420, 1482, 1326, 1215, 1012 cm^{-1}; ^1H NMR (400 MHz, $CDCl_3$) δ 7.90 (s, 1H), 7.47 (q, $J = 8.0$ Hz, 1H), 7.34 (d, $J = 8.0$ Hz, 1H), 7.29 (d, $J = 8.4$ Hz, 1H), 7.18–7.11 (m, 2H), 7.06 (d, $J = 2.4$ Hz, 1H), 6.96–6.90 (m, 3H), 3.78 (s, 3H), 1.95 (s, 6H); ^{13}C NMR (100 MHz, $CDCl_3$) δ 137.8, 137.1, 128.8, 126.7, 126.4, 125.6, 125.4, 124.0, 121.4, 121.3, 120.9, 120.6, 118.7, 118.1, 111.0, 109.2, 109.1, 100.9, 76.7, 34.9, 32.7, 30.2, 30.0; HRMS calcd for ($C_{20}H_{20}N_2$ + H^+) 289.1705, found: 289.1718 ($M + H^+$).

Data availability

The data supporting this article are available as part of the (ESI).†

Author contributions

S. M.—design and conceptualization; B. D.—catalyst preparation, reaction optimization, substrate scope and characterization; K. D.—synthesis of a few starting materials and substrate scope; UCD—theoretical calculations; S. M. and B. D—analysis of the spectral data and writing of the manuscript with input from other authors. All authors reviewed and approved the final version of manuscript.

Conflicts of interest

There are no conflicts to declare.

Acknowledgements

The authors gratefully acknowledge the Central Instrumental Centre (CIC), Tripura University, for the instrumental facility, and the Department of Science and Technology (DST), Government of India, for providing the 400 MHz NMR spectrometer through the DST-FIST programme (No. SR/FST/CSI-263/2015). BD acknowledges Tripura University for the non-NET fellowship.

References

1 (*a*) T. P. Singh and O. M. Singh, *Mini-Rev. Med. Chem.*, 2018, **18**, 9–25; (*b*) Y. Wan, Y. Li, C. Yan, M. Yan and Z. Tang, *Eur. J. Med. Chem.*, 2019, **183**, 111691; (*c*) M. Shiri, M. A. Zolfigol, H. G. Kruger and Z. Tanbakouchian, *Chem. Rev.*, 2010, **110**, 2250–2293; (*d*) M. Z. Zhang, Q. Chen and G. F. Yang, *Eur. J. Med. Chem.*, 2015, **89**, 421–441.

2 (*a*) M. Xia, S. Wang and W. B. Yuan, *Synth. Commun.*, 2004, **34**, 3175–3182; (*b*) M. Damodiran, D. Muralidharan and P. T. Perumal, *Bioorg. Med. Chem. Lett.*, 2009, **19**, 3611–3614; (*c*) A. J. K. Karamyan and M. T. Hamann, *Chem. Rev.*, 2010, **110**, 4489–4497; (*d*) M. Mari, A. Tassoni, S. Lucarini, M. Fanelli, G. Piersanti and G. Spadoni, *Eur. J. Org Chem.*, 2014, **2014**, 3822–3830.

3 (*a*) K. P. Pandey, M. T. Rahman and J. M. Cook, *Molecules*, 2021, **26**, 3459; (*b*) L. Khanna, Mansi, S. Yadav, N. Misra and P. Khanna, *Synth. Commun.*, 2021, **51**, 2892–2923.

4 (*a*) K. Rathi, O. S. Tiwari, V. Rawat, J. L. Jat, D. K. Yadav and V. P. Verma, *Org. Biomol. Chem.*, 2024, **22**, 3287–3298; (*b*) A. Nasreen, R. Varala and K. S. Rao, *Org. Commun.*, 2017, **10**, 104–113; (*c*) H. Veisi, R. Gholbedaghi, J. Malakootikhah, A. Sedrpoushan, B. Maleki and D. Kordestani, *J. Heterocycl. Chem.*, 2010, **47**, 1398–1405; (*d*) Z. Zheng, D. Zha, P. Cui, H. Zhang, C. Li, J. Shi and B. Han, *Results Chem.*, 2021, **3**, 100247.

5 M. Chakrabarty, N. Ghosh, R. Basak and Y. Harigaya, *Tetrahedron Lett.*, 2002, **43**, 4075–4078.

6 M. M. Heravi, K. Bakhtiari, A. Fatehi and F. F. Bamoharram, *Catal. Commun.*, 2008, **9**, 289–292.

7 R. S. Balaskar, B. B. Shingate, M. S. Shingare and D. V. Mane, *Arab. J. Chem.*, 2016, **9**, S120–S123.

8 P. J. Das and J. Das, *Tetrahedron Lett.*, 2012, **53**, 4718–4720.

9 B. L. Tornquist, D. P. G. Bueno, J. C. M. Willig, I. M. D. Oliveira, A. S. Helio, J. Rafique, S. Saba, B. A. Iglesias, G. V. Botteselle and F. Manarin, *ChemistrySelect*, 2018, **3**, 6358–6363.

10 S.-J. Ji, M.-F. Zhou, D.-G. Gu, S.-Y. Wang and T.-P. Loh, *Synlett*, 2003, 2077–2079.

11 A. Suárez, F. Martíne, S. Suárez-Pantiga and R. Sanz, *ChemistrySelect*, 2017, **1**, 1–5.

12 J. R. Satam, K. D. Parghi and R. V. Jayaram, *Catal. Commun.*, 2008, **9**, 1071–1078.

13 A. Z. Halimehjani and V. Barati, *ChemistrySelect*, 2018, **3**, 3024–3028.

14 R. M. N. Kalla, S. C. Hong and I. Kim, *ACS Omega*, 2018, **3**, 2242–2253.

15 P. Thirupathi and S. S. Kim, *J. Org. Chem.*, 2010, **75**, 5240–5249.

16 N. C. Ganguly, P. Mondal and S. K. Barik, *Green Chem. Lett. Rev.*, 2012, **5**, 73–81.

17 H. Lin, Y. Zang, X. Sun and G. Lin, *Chin. J. Chem.*, 2012, **30**, 2309–2314.

18 K. A. Chavan, M. Shukla, A. N. Singh Chauhan, S. Maji, G. Mali, S. Bhattacharyya and R. D. Erande, *ACS Omega*, 2022, **7**, 10438–10446.

19 S. R. Mendes, S. Thurow, F. Penteado, M. S. da Silva, R. A. Gariani, G. Perin and E. J. Lenardão, *Green Chem.*, 2015, **17**, 4334–4339.

20 M. Esmaielpour, B. Akhlaghinia and R. Jahanshahi, *J. Chem. Sci.*, 2017, **129**, 313–328.

21 N. A. Khalafi, M. Nourisefat and F. Panahi, *RSC Adv.*, 2014, **4**, 22497–22500.

22 C. Ramesh, J. Banerjee, R. Pal and B. Das, *Adv. Synth. Catal.*, 2003, **345**, 557–559.

23 B. Deb, S. Debnath, A. Chakraborty and S. Majumdar, *RSC Adv.*, 2021, **11**, 30827–30839.

24 Y.-S. Zhao, H.-L. Ruan, X.-Y. Wang, C. Chen, P.-F. Song, C.-W. Lü and L.-W. Zou, *RSC Adv.*, 2019, **9**, 40168–40175.

25 Z. B. Xie, D. Z. Sun, G. F. Jiang and Z. G. Le, *Molecules*, 2014, **19**, 19665–19677.

26 J. Xiao, H. Wen, L. Wang, L. Xu, Z. Hao, C.-L. Shao and C.-Y. Wang, *Green Chem.*, 2016, **18**, 1032–1037.

27 (*a*) J.-B. Peng, X. Qi and X.-F. Wu, *Synlett*, 2016, **28**, 175–194; (*b*) J.-B. Peng, X. Qi and X.-F. Wu, *ChemSusChem*, 2016, **9**, 2279–2283; (*c*) Y. Bai, D. C. Davis and M. Dai, *J. Org. Chem.*, 2017, **82**, 2319–2328.

28 (*a*) J. Jin, Y. Li, S. Xiang, W. Fan, S. Guo and D. Huang, *Org. Biomol. Chem.*, 2021, **19**, 4076–4081; (*b*) V. D. Kadu, S. N. Chandrudu, M. G. Hublikar, D. G. Raut and R. B. Bhosale, *RSC Adv.*, 2020, **10**, 23254–23262.

29 F. Stanek, R. Pawlowski, P. Morawska, R. Bujok and M. Stodulski, *Org. Biomol. Chem.*, 2020, **18**, 2103–2112.

30 P. Saini, P. Kumari, S. Hazra and A. J. Elias, *Chem.–Asian J.*, 2019, **14**, 4154–4159.

31 N.-K. Nguyen, M.-T. Ha, H. Y. Bui, Q. T. Trinh, B. N. Tran, V. T. Nguyen, T. Q. Hung, T. T. Dang and X. H. Vu, *Catal. Commun.*, 2021, **149**, 106240.

32 T. Pillaiyar, E. Gorska, G. Schnakenburg and C. E. Müller, *J. Org. Chem.*, 2018, **83**, 9902–9913.

33 A. Devi, M. M. Bharali, S. Biswas, T. J. Bora, J. K. Nath, S. Lee, Y.-B. Park, L. Saikia, M. J. Baruah and K. K. Bania, *Green Chem.*, 2023, **25**, 3443–3448.

34 E. M. Galathri, T. J. Kuczmera, B. J. Nachtsheim and C. G. Kokotos, *Green Chem.*, 2024, **26**, 825–831.

35 P. G. M. Wuts, *Greene's Protective Groups in Organic Synthesis*, John Wiley & Sons, Inc., Hoboken, New Jersey, 5th edn, 2014.

36 A. G. Volbeda, G. A. van der Marel and J. D. C. Codée, Protecting Group Strategies in Carbohydrate Chemistry, in *Protecting Groups – Strategies and Applications in*

Carbohydrate Chemistry, ed. S. Vidal, Wiley-VCH, Weinheim, 2019, pp. 1–28.

37 (*a*) D. D. Diaz, P. O. Miranda, J. I. Padron and V. S. Martin, *Curr. Org. Chem.*, 2006, **10**, 457–476; (*b*) M. Mishra, S. Mohapatra, N. P. Mishra, B. K. Jena, P. Panda and S. Nayak, *Tetrahedron Lett.*, 2019, **60**, 150925; (*c*) I. Bauer and H.-J. Knolker, *Chem. Rev.*, 2015, **115**, 3170–3387; (*d*) A. A. O. Sarhan and C. Bolm, *Chem. Soc. Rev.*, 2009, **38**, 2730–2744; (*e*) S. Ruengsangtongkul, P. Taprasert, U. Sirion and J. Jaratjaroonphong, *Org. Biomol. Chem.*, 2016, **14**, 8493–8502; (*f*) C. Chantana and J. Jaratjaroonphong, *J. Org. Chem.*, 2021, **86**, 2312–2327.

38 S.-J. Ji, M.-F. Zhou, D.-G. Gu, Z.-Q. Jiang and T.-P. Loh, *Euro. J. Org. Chem.*, 2004, 1584–1587.

39 V. Terrasson, J. Michaux, A. Gaucher, J. Wehbe, S. Marque, D. Prim and J.-M. Campagne, *Euro. J. Org. Chem.*, 2007, 5332–5335.

40 C. Fan, R. Li, J. Duan, K. Xu, Y. Liu, D. Wang and X. He, *Synth. Commun.*, 2022, **52**, 1155–1164.

41 S. Majumdar, A. Chakraborty, S. Bhattacharjee, S. Debnath and D. K. Maiti, *Tetrahedron Lett.*, 2016, **57**, 4595–4598.

42 (*a*) D. Habibi and M. Nasrollahzadeh, *Synth. Commun.*, 2010, **40**, 3159–3167; (*b*) M. A. Taher, C. Karami, M. S. Arabi, H. Ahmadian and Y. Karami, *Int. Nano Lett.*, 2016, **6**, 85–90; (*c*) E. Keinan and Y. Mazur, *J. Org. Chem.*, 1978, **43**, 1020–1022.

43 (*a*) S. E. Sen, S. L. Roach, J. K. Boggs, G. J. Ewing and J. Magrath, *J. Org. Chem.*, 1997, **62**(19), 6684–6686; (*b*) T. Xu, Q. Yang, D. Li, J. Dong, Z. Yu and Y. Li, *Chem.–Eur. J.*, 2010, **16**, 9264–9272.

44 (*a*) S. Ghosh, S. Khamarui, K. S. Gayen and D. K. Maiti, *Sci. Rep.*, 2013, **3**, 2987; (*b*) S. Ghosh, S. Debnath, U. K. Das and D. K. Maiti, *Ind. Eng. Chem. Res.*, 2017, **56**(42), 12056–12069.

45 (*a*) S. Majumdar, M. Chakraborty, D. K. Maiti, S. Chowdhury and J. Hossain, *RSC Adv.*, 2014, **4**, 16497–16502; (*b*) S. Majumdar, M. Chakraborty, N. Pramanik and D. K. Maiti, *RSC Adv.*, 2015, **5**, 51012–51018; (*c*) K. Das and S. Majumdar, *RSC Adv.*, 2022, **12**, 21493–21502; (*d*) A. Rudra Paul, S. Debnath and S. Majumdar, *ChemistrySelect*, 2023, **8**, e202300007; (*e*) A. Rudra Paul, S. Sarkar, J. Hossain, S. A. Hussain and S. Majumdar, *Res. Chem. Intermed.*, 2022, **48**, 4963–4985; (*f*) K. Das, B. Das, B. Paul, R. Natarajan and S. Majumdar, *Silicon*, 2024, **16**, 967–977.

46 B. Das, A. Bhattacharyya, B. Paul, R. Natarajan and S. Majumdar, *RSC Adv.*, 2024, **14**, 33512–33523.

47 M. J. Frisch, G. W. Trucks, H. B. Schlegel, G. E. Scuseria, *et al*, *Gaussian 16, Revision C.01*, Gaussian, Inc., Wallingford CT, 2019.

48 J.-I. Aihara, *J. Phys. Chem. A*, 1999, **103**, 7487–7495.

49 N. Blankevoort, P. Bastante, R. J. Davidson, R. J. Salthouse, A. H. S. Daaoub, P. Cea, S. M. Solans, A. S. Batsanov, S. Sangtarash, M. R. Bryce, N. Agrait and H. Sadeghi, *ACS Omega*, 2024, **9**, 8471–8477.

50 (*a*) S. Majumdar, A. Bhattacharjya and A. Patra, *Tetrahedron*, 1999, **55**, 12157–12174; (*b*) G. V. M. Sharma, I. S. Reddy, V. G. Reddy and A. V. Rama Rao, *Tetrahedron: Asymmetry*, 1999, **10**, 229–235.